

# Chapter 1

## Amorphous and Nanocrystalline Glass-Coated Wires: Optimization of Soft Magnetic Properties

V. Zhukova, M. Ipatov, A. Talaat, J.M. Blanco, and Arcady Zhukov

### 1.1 Introduction

Soft magnetic wires presently considered as one of the most promising magnetic materials for industrial applications in various industrial sectors such as magnetic sensors, microelectronics, security and smart composites [1–7]. The main reason for this continuous interest is related to the possibility to obtain thin magnetic wires with extremely soft magnetic properties. Moreover magnetically soft microwire can also exhibit Giant Magnetoimpedance (GMI) effect that usually related to high circumferential magnetic permeability of magnetic wires [7–9]. Usually high magnetic permeability and GMI effect can be observed in magnetic wires with

---

V. Zhukova (✉) • M. Ipatov  
Department of Material Physics, Basque Country University, UPV/EHU,  
San Sebastian 20018, Spain

Departamento de Física Aplicada, EUPDS, Basque Country University,  
UPV/EHU, San Sebastian 20018, Spain  
e-mail: [valentina.zhukova@ehu.eus](mailto:valentina.zhukova@ehu.eus)

A. Talaat  
Department of Material Physics, Basque Country University, UPV/EHU,  
San Sebastian 20018, Spain

J.M. Blanco  
Departamento de Física Aplicada, EUPDS, Basque Country University,  
UPV/EHU, San Sebastian 20018, Spain

A. Zhukov  
Department of Material Physics, Basque Country University, UPV/EHU,  
San Sebastian 20018, Spain

Departamento de Física Aplicada, EUPDS, Basque Country University,  
UPV/EHU, San Sebastian 20018, Spain

IKERBASQUE, Basque Foundation for Science, Bilbao, Spain

vanishing magnetostriction coefficient [7–9]. Moreover amorphous character of magnetic wires prepared using rapidly quenching technique allows achievement of magnetic softness.

Phenomenologically the aforementioned GMI effect consists of large change of the impedance of magnetically soft conductor on applied magnetic field. GMI effect has been successfully explained in the terms of classical electrodynamics through the influence of magnetic field on penetration depth of electrical current flowing through the magnetically soft conductor [7–10].

Usually for characterization of the GMI effect the magneto impedance ratio,  $\Delta Z/Z$ , is used. The aforementioned GMI ratio,  $\Delta Z/Z$ , is defined as:

$$\Delta Z/Z = [Z(H) - Z(H_{\max})]/Z(H_{\max}), \quad (1.1)$$

where  $H_{\max}$  is the axial DC-field with maximum value up to few kA/m.

It is worth mentioning that, although discovery of the GMI effect has been attributed to first papers on amorphous wires where GMI effect has been described and explained [9, 10], the GMI effect has been described in 1930 in permalloy soft magnetic wire [7].

On the other hand, the other family of magnetic wires (basically with non-zero magnetostriction coefficient) can exhibit rectangular hysteresis loops. In this family of microwires the remagnetization process runs by the fast domain walls propagation along the wire [11–13]. Fast and controllable domain wall (DW) propagation in various families of magnetic wires has been proposed for quite promising applications in micro- and nanotechnology (magnetic memory, magnetic logic, magnetic TAGs, etc.) [14, 15].

In the case of glass-coated amorphous microwires exhibiting spontaneous magnetic bistability the DW propagation with a speed above 1 km/s can be easily achieved [11–13]. Therefore studies of DW dynamics in amorphous glass-coated microwires are quite important for understanding of the origin of fast DW propagation and ways to enhance the DW velocity in other materials.

Additionally a miniaturization of magnetic sensors allows reduction of the materials consumption and permits to find out new applications. Such trend in sensors miniaturization requires development of magnetic wires with reduced diameters [2, 3, 8].

Consequently studies of thin magnetically soft wires with enhanced magnetic softness, GMI effect and fast magnetization switching exhibiting rapid DW propagation attract attention during last two decades [8].

Up to know the thinnest magnetic wires are reported when utilizing the so-called Taylor–Ulitovsky method allowing preparation of glass-coated microwires with metallic nucleus diameters from 0.05 to 50  $\mu\text{m}$  coated by glass with thickness ranging from 0.5 up to 30  $\mu\text{m}$  [4]. The fabrication method essentially consists of the melting of the metallic alloy ingot inside the glass tube, forming the glass capillary and rapid quenching from the melt of the metallic nucleus completely coated by a glass [3, 16].

It is worth mentioning that although glass-coated microwires attracted interest during last two decades, the fabrication method is known along many years [17–21]. Initially the method for fabrication of glass-coated microwires has been introduced by Taylor [17]. Later it was modified by Ulitovsky. The modified method allowed preparation of long glass-coated microwires (the main modification was the introduction of the rotating bobbins that permitted to considerably enhance the length of glass-coated microwire). Initially this method has been developed for the preparation of Cu and Ag non-magnetic glass-coated microwires [17, 18]. Later few successful attempts of fabrication of Fe-based magnetic amorphous microwires have been reported in East Europe [19–21]. Thus considerable effect of annealing on hysteresis loop of FeP microwires and rectangular hysteresis loop in FeNiPB glass-coated microwires has been observed [22, 23].

The interest in thin magnetic wires was stimulated at the beginning of 1990 after reports on GMI effect in soft magnetic amorphous wires [9, 10] and proposed applications of the GMI effect in magnetic microsensors [6]. Consequently a number of papers on optimization of magnetic properties of glass-coated microwires have been published after 1995 [2–5, 24].

One of the features of the fabrication method is considerable difference of the thermal expansion coefficients of the glass and the metal results in appearance of considerable internal stresses [2–5, 16, 24]. These internal stresses considerably affect soft magnetic properties of amorphous materials [16]. Therefore in amorphous microwire (i.e. in the absence of magnetocrystalline anisotropy) the magnetoelastic anisotropy becomes the main factor that affects magnetic properties of glass-coated microwires.

The other important factor that affects soft magnetic properties of amorphous materials is the shape anisotropy. But in micrometric magnetic wires the influence of demagnetizing factor becomes negligible for the wire length below few mm.

Consequently, the main attention for engineering of magnetic properties of glass-coated microwires must be paid to the magnetoelastic anisotropy requires. The aforementioned magnetoelastic energy is essentially determined by the magnetostriction coefficient,  $\lambda_s$ , and internal stresses,  $\sigma_i$ :

$$K_{me} \approx 3/2\lambda_s\sigma_i, \quad (1.2)$$

The magnetostriction constant depends mostly on the chemical composition and is vanishing in amorphous Fe–Co-based alloys with Co/Fe  $\approx$  70/5 [25–27].

Consequently main possibilities to tailor magnetic properties of amorphous microwires are either internal stress or selection of the appropriate chemical composition of the metallic nucleus [16]. Internal stresses in principle can be modified by few different ways, i.e., by:

- Heat treatment
- Chemical etching or mechanical removal of the glass coating or
- Controlling of the stresses through the modification of the ratio,  $\rho$ , between the metallic nucleus diameter,  $d$  and total microwire diameter,  $D(\rho = d/D)$ .

On the other hand, the alternative way of engineering of magnetic properties of magnetic microwires is controllable crystallization. It is well known that, the so-called nanocrystalline materials, i.e., two-phase materials consisting of nano-sized crystallites embedded in an amorphous matrix can exhibit extremely soft magnetic properties.

Nanocrystalline magnetic materials are known since 1988, when for the first time was reported that the presence of small additions of Cu and Nb in FeSiB-based alloys allows the obtaining of a two-phase material by the devitrification of the amorphous alloy after adequate annealing (i.e. at temperatures between the first and second crystallization processes) [28–30]. After first stage of crystallization, nanocrystalline material consists of small (around 10 nm) nanocrystallites embedded in the residual amorphous matrix.

Magnetic softness of nanocrystalline materials is thought to be originated by vanishing of the magnetocrystalline anisotropy (also known as a random anisotropy model) as well as by quite low magnetostriction constant of the two-phase materials when the grain size approaches 10 nm [29–31].

Recently successful attempts of improvement of magnetic softness and the GMI effect of thin magnetic wires by nanocrystallization of amorphous precursor have been reported [32–37].

In fact substitution of Co-rich amorphous microwires by less expensive Fe-rich microwires can be essentially promising from industrial application's point of view. Therefore, optimizing high GMI effect in Fe-rich glass-coated microwires is important from the viewpoint of the massive applications.

In this chapter we present our last results on optimization of GMI effect in amorphous and nanocrystalline glass-coated microwires.

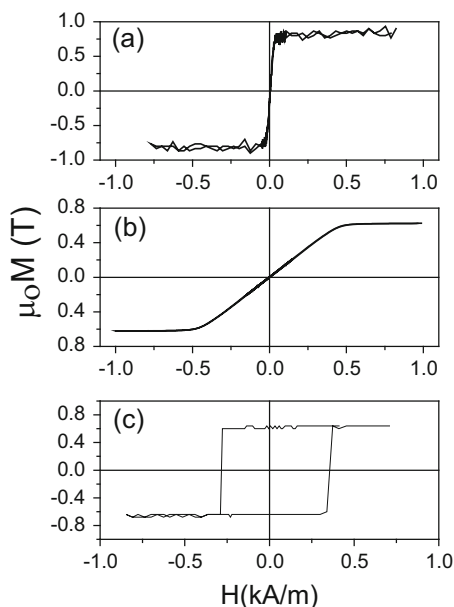
## 1.2 Engineering of Magnetic Properties and GMI Effect of Amorphous Microwires

Magnetic properties of glass-coated microwires essentially depend on chemical composition of the metallic nucleus [8]. The most drastic changes of the hysteresis loop have been reported for the  $\text{Co}_x\text{Fe}_{1-x}$  ( $0 \leq x \leq 1$ ) system [8, 24]. This compositional dependence is attributed to the change of the magnetostriction coefficient in the Co–Fe-based microwires [25–27]. As mentioned above in classical amorphous materials  $(\text{Co}_x\text{Fe}_{1-x})_{75}\text{Si}_{15}\text{B}_{10}$  the magnetostriction coefficient,  $\lambda_s$ , changes with  $x$  from  $-5 \times 10^{-6}$  at  $x = 1$ , to  $\lambda_s \approx 35 \times 10^{-6}$  at  $x \approx 0.2$ , achieving nearly zero values at Co/Fe about 70/5.

Consequently best soft magnetic properties are observed for nearly zero magnetostrictive Co-rich compositions (Co/Fe around 70/5).

On the other hand, microwires with Fe-rich metallic nucleus composition present rather different magnetic properties exhibiting rectangular hysteresis loops related with large and single Barkhausen jump.

**Fig. 1.1** Hysteresis loop of amorphous Co-rich microwires with nearly zero magnetostriction (a) and negative magnetostriction (b) coefficients and Fe-rich microwire with positive magnetostriction (c)



In contrast to the Fe-rich glass-coated microwires presenting perfectly rectangular (usually also called as bistable) hysteresis loops, Co-rich amorphous microwires with negative magnetostriction coefficient exhibit nearly non-hysteretic behaviour [38]. In particular, hysteresis loops of magnetic microwires with nearly zero magnetostrictive compositions exhibit very low coercivities and quite large initial susceptibility [8].

Consequently generally magnetic properties and overall shape of hysteresis loops of amorphous microwires depend on composition of the metallic nucleus as well as on composition and thickness of the glass coating [39, 40, 41]. This can be illustrated by Fig. 1.1, where the hysteresis loops of three main groups of amorphous microwires (Fe-rich, Co-rich and Co-Fe-rich with positive, negative and vanishing magnetostriction constant, respectively) are shown.

Therefore the most common way for tailoring of the magnetic properties is the proper chemical composition selection.

But for further tuning of the properties the internal stresses can be taken into account.

As mentioned above, the internal stresses,  $\sigma_i$ , arising during simultaneous rapid quenching of metallic nucleus surrounding by the glass coating are the source of additionally magnetoelastic anisotropy. The strength of such internal stresses can be controlled by the  $\rho$ -ratio: strength of internal stresses increases decreasing  $\rho$ -ratio (i.e. increases with increasing of the glass volume) [40–43].

Consequently in each family of compositions the internal stresses influence is the other factor that affects the magnetic properties of microwires.

This influence is illustrated in Figs. 1.2 and 1.3.

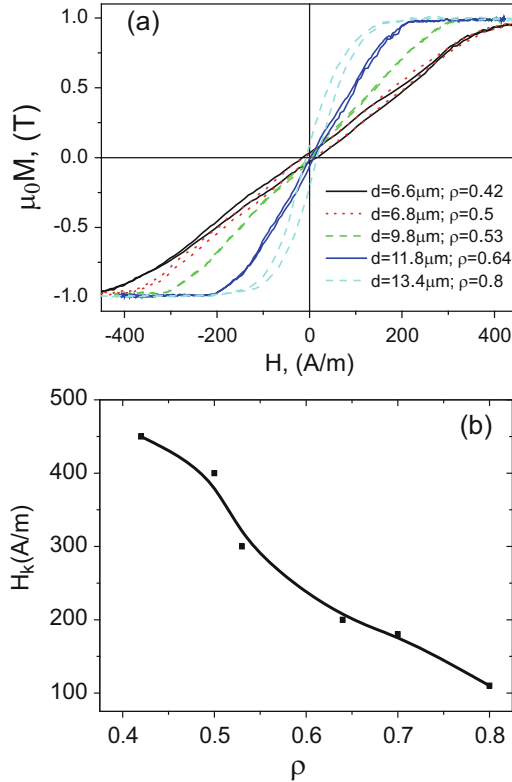


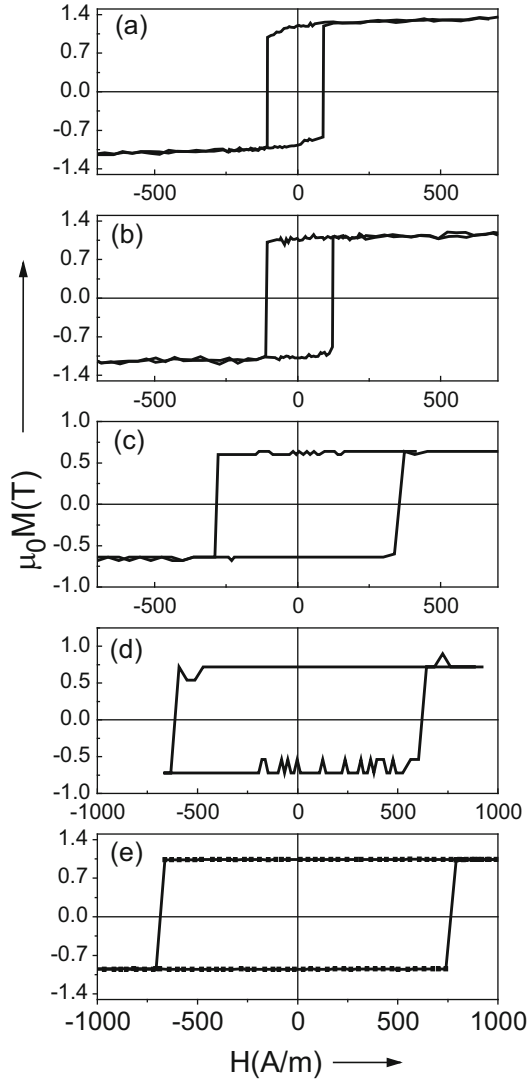
**Fig. 1.2** Hysteresis loops of  $\text{Co}_{67.1}\text{Fe}_{3.8}\text{Ni}_{1.4}\text{Si}_{14.5}\text{B}_{11.5}\text{Mo}_{1.7}$  microwires with different geometry (a) and dependence of  $H_k$  on  $\rho$ -ratio (b). Reprinted with permission from [45], A. Zhukov, M. Ipatov and V. Zhukova “Amorphous microwires with enhanced magnetic softness and GMI characteristics” EPJ Web of Conferences **29** 00052 (2012) DOI: 10.1051/ Owned by the authors, published by EDP Sciences, 2012 (Fig. 4)

Particularly the influence of the internal stresses on hysteresis loops of Co-rich (with vanishing  $\lambda_s$ -values) and Fe-rich (with positive  $\lambda_s$ -values) are shown in Figs. 1.2 and 1.3, where hysteresis loops of both families of microwires of the same chemical composition but with different  $\rho$ -ratios (different internal stresses) are shown.

The estimated values of the internal stresses in these glass-coated microwires arising from the difference in the thermal expansion coefficients of metallic nucleus and glass coating are of the order of 100–1000 MPa, depending strongly on the  $\rho$ -ratio [42–44], increasing with the glass coating thickness.

Such large internal stresses give rise to a drastic change of the magnetoelastic energy,  $K_{\text{me}}$ , given by Eq. (1.2) even for small changes of the glass-coating thickness at fixed metallic core diameter. Additionally, such a change of the  $\rho$ -

**Fig. 1.3** Hysteresis loops of Fe-rich amorphous microwires with the same sample length and different metallic nucleus diameter  $d$  and total diameters  $D$ :  $\text{Fe}_{70}\text{B}_{15}\text{Si}_{10}\text{C}_5$  microwires with  $\rho = 0.63$ ;  $d = 15 \mu\text{m}$  (a);  $\rho = 0.48$ ;  $d = 10.8 \mu\text{m}$  (b);  $\rho = 0.26$ ;  $d = 6 \mu\text{m}$  (c);  $\rho = 0.16$ ;  $d = 3 \mu\text{m}$  (d) and of  $\text{Fe}_{72.75}\text{Co}_{2.25}\text{B}_{15}\text{Si}_{10}$  microwire with  $\rho = 0.14$ ;  $d \approx 1.4 \mu\text{m}$  (e). Reprinted with permission from [46]. Copyright (2012) SpringerOpen (Fig. 1)



ratio should be related to the change of the magnetostriction constant with stresses,  $\sigma$  (either applied or internal) [45, 46]:

$$\lambda_s = (\mu_o M_\sigma / 3) (d_\kappa / d\sigma) \tag{1.3}$$

where  $\mu_o M_s$  is the saturation magnetization.

It is worth mentioning that residual stresses of glass-coated microwires arising during simultaneous solidification of metallic nucleus and glass coating, mostly have been estimated from the simulations of the process of simultaneous

solidification of metallic nucleus inside the glass tube [42–44] and experimental determination of such residual stresses is rather complex. In according to the simulation results these stresses present tensor character and the strongest stresses in most part of metallic nucleus value are the tensile stresses [42, 43].

Experimentally evidence of internal stresses is the dependence of hysteresis loops and particularly of magnetic properties (coercivity, remanent magnetization) on  $\rho$ -ratio [45, 46] as well as the applied stress dependence of the hysteresis loops [47–50] and effect of chemical etching of the glass on hysteresis loops [51, 52]. As can be appreciated from Fig. 1.3, considerable increasing of coercivity,  $H_c$ , and switching field,  $H_s$ , with decreasing of  $\rho$ -ratio is observed.

Direct confirmation of the magnetoelastic origin of observed changes of the hysteresis loops is the dependence of the measured effect of the switching field,  $H_s$ , on applied stresses,  $\sigma_a$ . Switching field,  $H_s$ , is defined as the field at which the large Barkhausen jump starts. It is worth mentioning that at low magnetic field amplitudes and frequencies the  $H_s$  is almost as same as coercivity,  $H_c$ . But the switching field,  $H_s$ , is usually almost independent on magnetic field amplitude,  $H_0$  and frequency,  $f$  [53]. The difference between  $H_s$  and  $H_c$  was attributed to the DW dynamics, i.e., the time of domain wall propagation through the entire wire [54]. Therefore use of  $H_s$  for studying of stress dependence of hysteresis loops is more rigorous.

Similarly to the result presented in Fig. 1.3 a considerable and monotonic growth of  $H_s$  with  $\sigma_a$  is observed (Fig. 1.4). Consequently from comparison of Figs. 1.3 and 1.4 we can deduce that the internal stresses in glass-coated microwires are mostly of tensile origin and that the strength of internal stresses increase with  $\rho$ -ratio decreasing.

Similarly, after chemical etching of the glass coating we observed gradual changes of the hysteresis loop from almost unhysteretic and linear to almost rectangular in Co-rich microwires (Fig. 1.5).

**Fig. 1.4** Effect of applied stresses on switching field of  $\text{Fe}_{70}\text{B}_{15}\text{Si}_{10}\text{C}_5$  amorphous microwires with the different  $\rho$ -ratio:  $\rho = 0.63$ ,  $d = 15 \mu\text{m}$  and  $\rho = 0.48$ ,  $d = 10.8 \mu\text{m}$ . Reprinted with permission from [50]

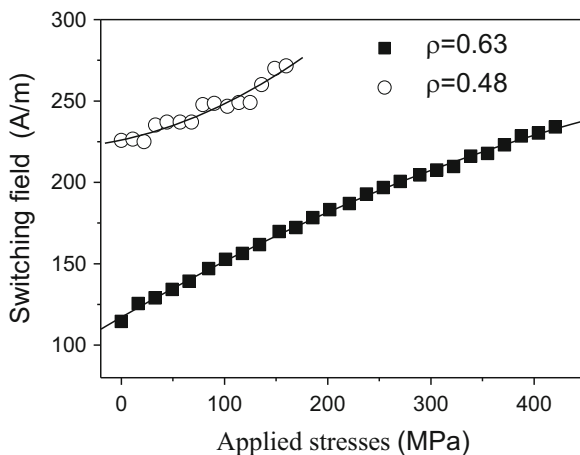
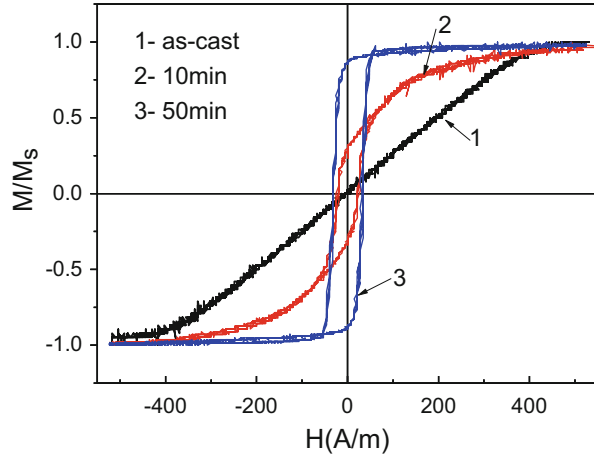




**Fig. 1.5** Hysteresis loops of  $\text{Co}_{70.5}\text{Mn}_{4.5}\text{Si}_{10}\text{B}_{15}$  microwire in the as-cast state (1) and chemically treated during 10 min (2) and 50 min (3)



Moreover quite recently we observed similar tendency after annealing of Co-rich microwires: annealing considerably affects magnetic properties of Co-rich microwires. Hysteresis loops becomes almost rectangular after annealing (see Fig. 1.6). As shown in Fig. 1.6 upon increasing the annealing time at fixed annealing temperature (250 °C in Fig. 1.6) the hysteresis loops become more and more rectangular. A similar tendency has been observed at different annealing temperatures [54, 55].

Consequently non-magnetic glass coating affects the hysteresis loops of ferromagnetic nucleus through the internal stresses induced by the glass coating inside the metallic nucleus.

Therefore, tailoring of the magnetoelastic energy,  $K_{me}$ , is essentially important for optimization of magnetic properties of glass-coated microwires [45–52].

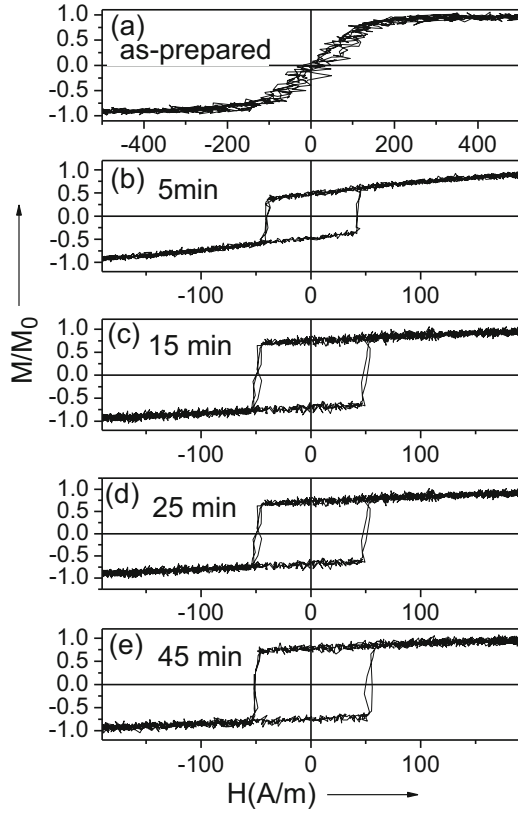
GMI effect is the highest in magnetically soft materials, i.e., in materials with high magnetic permeability. It is worth mentioning that the DC magnetic field dependence of GMI effect in magnetic materials with transverse magnetic anisotropy presents a maximum. The DC magnetic field that corresponds to the maximum GMI ratio,  $H_m$ , is attributed to the static magnetic anisotropy field,  $H_k$ . Consequently, there is close relation between the magnetic softness and magnetic field dependence of the GMI effect.

Moreover the parameter  $\rho$  must be considered as one of the factors that affect both soft magnetic properties and GMI of glass-coated microwires.

The influence of the  $\rho$ -ratio on GMI ratio and on  $\Delta Z/Z$  magnetic field dependence is reported elsewhere [8, 41].

As can be appreciated,  $\text{Co}_{67.1}\text{Fe}_{3.8}\text{Ni}_{1.4}\text{Si}_{14.5}\text{B}_{11.5}$  microwire with appropriate geometry and composition presents excellent magnetically soft properties with low coercivities (between 4 and 10 A/m, see Fig. 1.2) [8]. Magnetic anisotropy field,  $H_k$ , is found to be determined by the  $\rho$ -ratio, decreasing with  $\rho$  (Fig. 1.2b), as reported elsewhere [8, 41].

**Fig. 1.6** Effect of annealing time on hysteresis loops of  $\text{Co}_{69.2}\text{Fe}_{4.1}\text{B}_{11.8}\text{Si}_{13.8}\text{C}_{1.1}$  microwires annealed at  $T_{\text{ann}} = 250^\circ\text{C}$ . Reprinted with permission from [55], Fig. 6



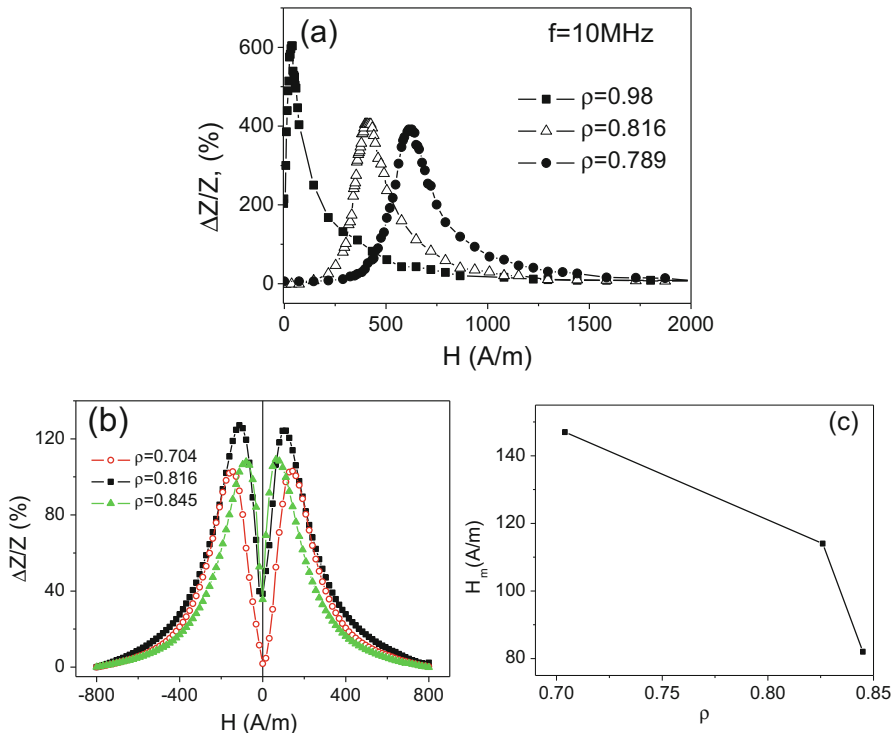
Consequently, one can expect that the  $\rho$ -ratio must affect the GMI effect of studied samples.

Figure 1.7 presents results on magnetic field dependences of  $\Delta Z/Z$  measured in  $\text{Co}_{67.05}\text{Fe}_{3.85}\text{Ni}_{1.4}\text{B}_{11.33}\text{Si}_{14.47}\text{Mo}_{1.69}$  microwire samples with different  $\rho$ -ratios.

Indeed both maximum values of the GMI ratio,  $\Delta Z/Z_m$ , and the magnetic anisotropy field present considerable dependence on samples geometry. It is worth mentioning that for microwires with lowest glass coating thickness (largest  $\rho$ -ratio)  $\Delta Z/Z_m \approx 600\%$  has been observed [41].

Heat treatment is the usual way to relax the internal stresses. Therefore heat treatment is the other factor that considerably affects the GMI effect. As an example, the influence of current annealing on GMI ratio of Co-rich microwires is presented in Fig. 1.8. As can be seen from Fig. 1.8 after current annealing GMI ratio of  $\text{Co}_{67}\text{Fe}_{3.85}\text{Ni}_{1.45}\text{B}_{11.5}\text{Si}_{14.5}\text{Mo}_{1.7}$  microwire considerably increased [56].

On the other hand, heat treatment is not the method that always allows improvement of the GMI effect. Recently the influence of annealing on GMI effect of  $\text{Co}_{69.2}\text{Fe}_{4.1}\text{B}_{11.8}\text{Si}_{13.8}\text{C}_{1.1}$  microwires has been reported.



**Fig. 1.7** Effect of  $\rho$ -ratio on GMI effect in  $\text{Co}_{67.05}\text{Fe}_{3.85}\text{Ni}_{1.4}\text{B}_{11.33}\text{Si}_{14.47}\text{Mo}_{1.69}$  microwire samples with different  $\rho$ -ratios ((a), (b)) and dependence of field of maximums on  $\rho$ -ratio (c). Reprinted with permission from [41], V. Zhukova et al. “Optimization of Giant Magnetoimpedance in Co-Rich Amorphous Microwires” IEEE Trans. Magn., V 38, 5 part I, 2002 pp. 3090-3092. Copyright (2002) with permission from IEEE (Figure 4) and [7], A. Zhukov, M. Ipatov, M. Churyukanova, S. Kaloshkin, V. Zhukova, “Giant magnetoimpedance in thin amorphous wires: From manipulation of magnetic field dependence to industrial applications”, J. Alloys Comp. 586 (2014) S279–S286. Copyright (2014) with permission from Elsevier (Figure 4a)

The aforementioned Co-rich microwires with low coercivity usually present high GMI effect. As an example, as-prepared  $\text{Co}_{69.2}\text{Fe}_{4.1}\text{B}_{11.8}\text{Si}_{13.8}\text{C}_{1.1}$  amorphous microwires present soft magnetic behaviour with very low coercivity,  $H_c$  (about 8 A/m, see Fig. 1.9) and consequently high GMI ratio.

As mentioned above annealing considerably affects magnetic properties of studied samples: hysteresis loops becomes almost rectangular after annealing temperature (see Fig. 1.6).

GMI effect has been measured in as-prepared and annealed at  $300\text{ }^\circ\text{C}$  for 5 min  $\text{Co}_{69.2}\text{Fe}_{4.1}\text{B}_{11.8}\text{Si}_{13.8}\text{C}_{1.1}$  samples. After annealing of  $\text{Co}_{69.2}\text{Fe}_{4.1}\text{B}_{11.8}\text{Si}_{13.8}\text{C}_{1.1}$  microwire at this conditions present rectangular hysteresis loop but still with considerable magnetic permeability of the flat branches of the hysteresis loop (Fig. 1.10a). As can be appreciated from Fig. 1.10 the GMI ratio of annealed sample

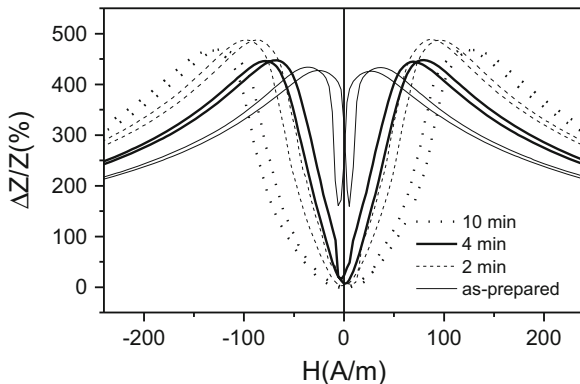


**Fig. 1.8**  $\Delta Z/Z(H)$  dependences of  $\text{Co}_{67}\text{Fe}_{3.85}\text{Ni}_{1.45}\text{B}_{11.5}\text{Si}_{14.5}\text{Mo}_{1.7}$  microwire measured at  $f = 30$  MHz and  $I = 1$  mA subjected to current annealing at 40 mA for different time. Reprinted with permission from [56], V. Zhukova, M. Ipatov, C. García, J. Gonzalez, J. M. Blanco and A. Zhukov, "Development of Ultra-Thin Glass-Coated Amorphous Microwires for High Frequency Magnetic Sensors Applications", *Open Materials Science Reviews*, 1,(2007), pp.1-12

**Fig. 1.9** Hysteresis loops (a) and  $\Delta Z/Z(H)$  dependence (b) measured at 100 MHz in as-prepared  $\text{Co}_{69.2}\text{Fe}_{4.1}\text{B}_{11.8}\text{Si}_{13.8}\text{C}_{1.1}$  microwire

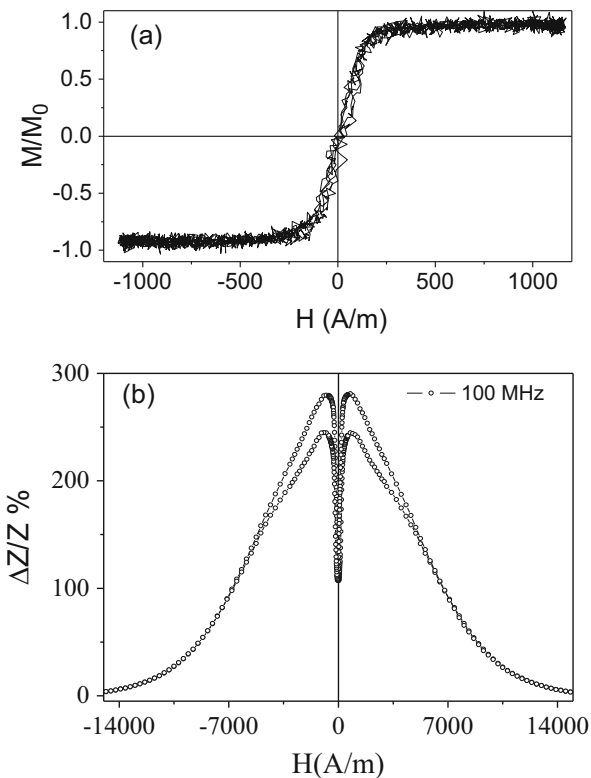
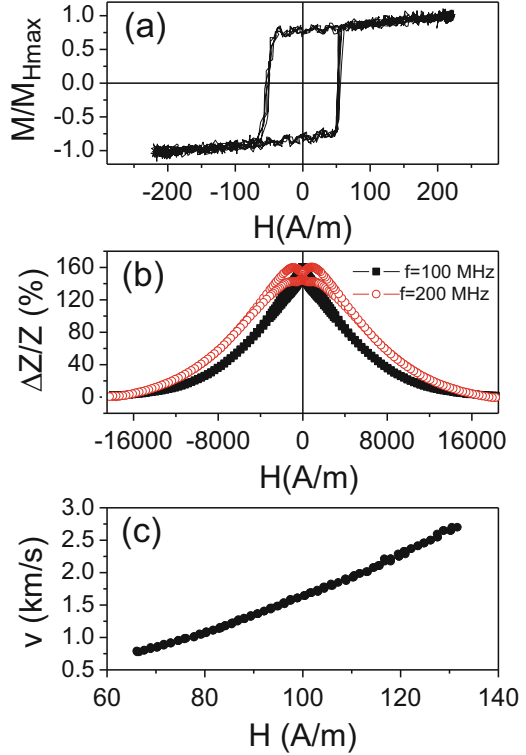


**Fig. 1.10** Hysteresis loop (a) magnetic field dependence of the GMI ratio (b) and  $v(H)$  dependence (c) measured in of annealed at 300 °C for 5 min  $\text{Co}_{69.2}\text{Fe}_{4.1}\text{B}_{11.8}\text{Si}_{13.8}\text{C}_{1.1}$  microwires



at 300 °C for 5 min is lower than in as-prepared microwire ( $\Delta Z/Z \approx 160$  %). Additionally a change of the magnetic field dependence of  $\Delta Z/Z$  is observed: the field for maximum GMI is lower in the annealed microwire for all measured frequencies. As discussed elsewhere, the field for maximum GMI corresponds to the magnetic anisotropy field [45]. Additionally the magnetic field dependence of the GMI ratio is strongly affected by magnetic anisotropy [45].

On the other hand, the same sample presents also quite fast single domain wall propagation: we observed typical single wall propagation with nearly linear growth of velocity  $v$  with magnetic field,  $H$ . The maximum velocity observed in this sample was about 2.5 km/s (Fig. 1.10c).

As-compared with results reported in literature, the magnitudes of the GMI ratio and domain wall velocity presently studied in our microwire exhibit similar values of GMI ratio values (maximum value about 300 %) in the as-prepared state. After annealing the maximum value of the GMI ratio decreases almost twice (from 300 % to about 160 %) but still remains reasonable for practical applications. On the other hand, maximum wall velocity observed in our annealed sample is quite high (about 2.5 km/s) being similar to that reported for microwires with low and positive magnetostriction value [19, 41].

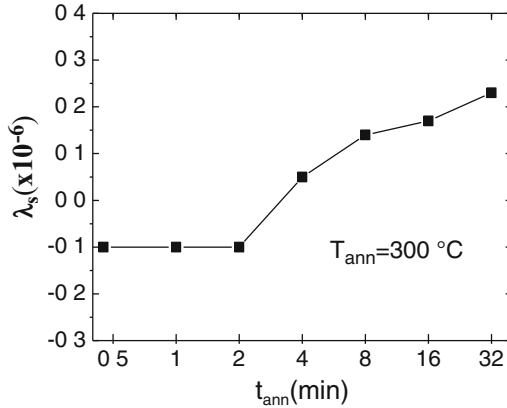


**Fig. 1.11** Effect of annealing conditions on magnetostriction,  $\lambda_s$  of  $\text{Fe}_{3.83}\text{Co}_{66.94}\text{Ni}_{1.44}\text{B}_{11.51}\text{Si}_{14.59}\text{Mo}_{1.69}$  microwires. Reprinted with permission from [57]

From the observed dependences we deduce that annealing induces an axial magnetic anisotropy.

But considerable GMI effect has been attributed to circular domain structure near the surface of annealed samples.

For explanation of the observed dependences few parallel phenomena have been proposed:

1. Effect of stress relaxation associated with the annealing affects the magnetostriction coefficient. Indeed recently direct measurements confirmed that considerable changes of the magnetostriction coefficient take place (see Fig. 1.11) [26, 57].
2. Tensile stress applied during annealing creates “back” stresses reducing the magnetostriction constant. Such “back” stresses have been considered for explanation of stress-induced anisotropy of Fe-rich microwires [58].

Perfectly rectangular hysteresis loops of Co-rich microwires observed after annealing (Fig. 1.10a) are quite similar to hysteresis loops of as-prepared Fe-rich microwires (Fig. 1.3): they exhibit similar coercivities and reducing the magnetic field amplitude below the switching field the hysteresis loop disappeared. Consequently we must assume that after annealing of Co-rich microwires we observe induced magnetic bistability.

Typical feature of microwires presenting magnetic bistability is the fast DW propagation within the inner axially magnetized core responsible for rectangular hysteresis loop.

Usually it is assumed that domain wall (DW) propagates along the wire with a velocity:

$$v = S(H - H_0) \quad (1.4)$$

where  $S$  is the DW mobility,  $H$  is the axial magnetic field and  $H_0$  is the critical propagation field.

In previous papers on studies of DW dynamics in microwires exhibiting spontaneous magnetic bistability there are few typical features.

### 1.2.1 Domain Wall Dynamics Is Affected by the Internal Stresses

As the example, dependences of the DW velocity,  $v$ , on magnetic field,  $H$  for  $\text{Fe}_{16}\text{Co}_{60}\text{Si}_{13}\text{B}_{11}$  and  $\text{Co}_{41.7}\text{Fe}_{36.4}\text{Si}_{10.1}\text{B}_{11.8}$  amorphous microwires with the same  $\rho$ -ratio but with different magnetostriction coefficients are shown in Fig. 1.12. In this case, the effect of only magnetostriction constant is that higher magnetostriction constant (in according to [25–27] for  $\text{Co}_{41.7}\text{Fe}_{36.4}\text{Si}_{10.1}\text{B}_{11}$  microwire  $\lambda_s \approx 30 \times 10^{-6}$  should be considered, while for  $\text{Fe}_{16}\text{Co}_{60}\text{Si}_{13}\text{B}_{11}$  composition  $\lambda_s \approx 15 \times 10^{-6}$ ) results in smaller DW velocity at the same magnetic field and smaller DW mobility,  $S$ .

In order to evaluate the effect of  $\rho$ -ratio, i.e., effect of residual stresses on DW dynamics, measurements of  $v(H)$  dependences in the microwires with the same composition but with different  $\rho$ -ratios have been performed. Dependences of DW velocity on applied field for  $\text{Fe}_{55}\text{Co}_{23}\text{B}_{11.8}\text{Si}_{10.1}$  microwires with different ratios are shown in Fig. 1.13. Like in Fig. 1.12, at the same values of applied field,  $H$ , the domain wall velocity is higher for microwires with higher  $\rho$ -ratio, i.e., when the internal stresses are lower [46].

Additionally to evaluate the magnetoelastic contribution the  $v(H)$  dependences under applied stresses have been measured. Observed  $v(H)$  dependences for

**Fig. 1.12**  $v(H)$  dependences for  $\text{Fe}_{16}\text{Co}_{60}\text{Si}_{13}\text{B}_{11}$  and  $\text{Co}_{41.7}\text{Fe}_{36.4}\text{Si}_{10.1}\text{B}_{11.8}$  microwires with  $\rho = 0.39$ .

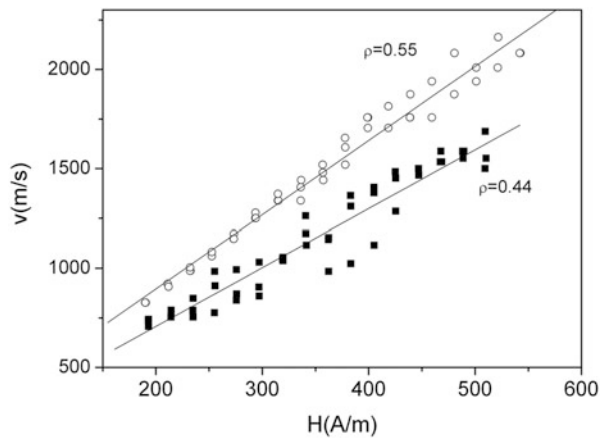


**Fig. 1.13**  $v(H)$  dependences for  $\text{Fe}_{35}\text{Co}_{23}\text{B}_{11.8}\text{Si}_{10.1}$  microwires with different ratios  $\rho$ . Reprinted with permission from [46]

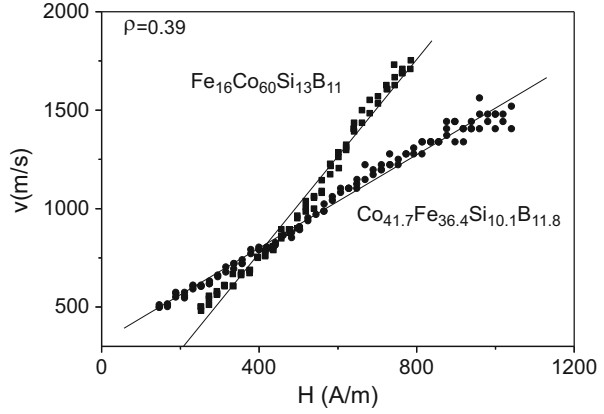
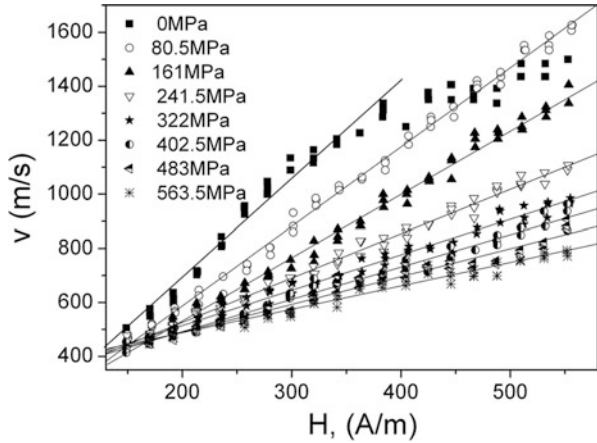


**Fig. 1.14**  $v(H)$  dependences for  $\text{Co}_{41.7}\text{Fe}_{36.4}\text{Si}_{10.1}\text{B}_{11.8}$  microwires ( $d \approx 13.6 \mu\text{m}$ ,  $D \approx 24.6 \mu\text{m}$ ,  $\rho \approx 0.55$ ) measured under application of applied stresses,  $\sigma_a$ . Reprinted with permission from [46]



$\text{Co}_{41.7}\text{Fe}_{36.4}\text{Si}_{10.1}\text{B}_{11.8}$  microwire ( $\rho \approx 0.55$ ) under applied stresses (see Fig. 1.14) present considerable decreasing of domain wall velocity,  $v$ , at the same magnetic field value,  $H$ , under application of applied stress. Additionally, increasing of applied stress,  $\sigma_a$ , results in decreasing of DW velocity.

Finally  $v(H)$  dependences in low magnetostrictive  $\text{Co}_{56}\text{Fe}_8\text{Ni}_{10}\text{Si}_{10}\text{B}_{16}$  microwire present considerable higher (almost twice) DW velocities than observed for microwires with higher magnetostriction constant DW at the same values of applied field (see Fig. 1.15).

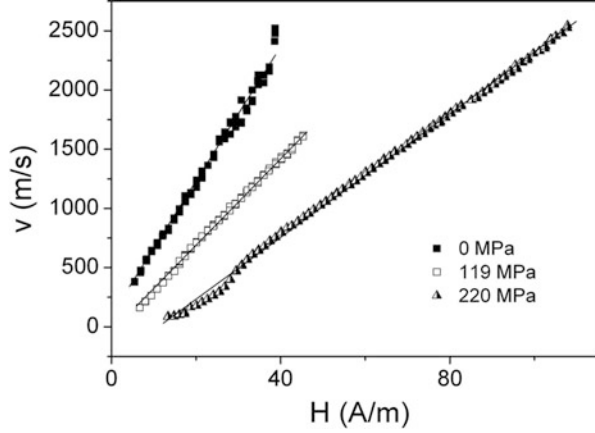
The domain wall dynamics in viscous regime is determined by a mobility relation (1.4), where  $S$  is the domain wall mobility given by:

$$S = 2\mu_0 M_s / \beta \quad (1.5)$$

where  $\beta$  is the viscous damping coefficient,  $\mu_0$  is magnetic permeability of vacuum. Damping is the most relevant parameter determining the domain wall dynamics.



**Fig. 1.15**  $v(H)$  dependences for  $\text{Co}_{56}\text{Fe}_8\text{Ni}_{10}\text{Si}_{10}\text{B}_{16}$  microwires measured under application of applied stresses,  $\sigma_a$ . Reprinted with permission from [46]



Various contributions to viscous damping  $\beta$  have been considered and two of them are generally accepted [46]:

- Micro-eddy currents circulating nearby moving domain wall are the more obvious cause of damping in metals. However, the eddy current parameter  $\beta_e$  is considered to be negligible in high-resistive materials, like thin amorphous microwires.

The second generally accepted contribution of energy dissipation is magnetic relaxation damping,  $\beta_r$ , related to a delayed rotation of electron spins. This damping is related to the Gilbert damping parameter and is inversely proportional to the domain wall width  $\delta_w$  [46],

$$\beta_r \approx \alpha M_s / \gamma \Delta \approx M_s (K_{\text{me}} / A)^{1/2} \quad (1.6)$$

where  $\gamma$  is the gyromagnetic ratio,  $A$  is the exchange stiffness constant,  $K_{\text{me}}$  is the magnetoelastic anisotropy.

Consequently, we can assume that the magnetoelastic energy can affect domain wall mobility,  $S$ , as we experimentally observed in few Co–Fe-rich microwires.

In the case of only the magnetoelastic origin of the stress dependence of DW velocity,  $v$ , this dependence should exhibit an inverse square root dependence. In Fig. 1.16 we present our attempt to evaluate quantitatively observed  $v(\sigma_a)$  dependence for  $\text{Fe}_{55}\text{Co}_{23}\text{B}_{11.8}\text{Si}_{10.2}$  microwires ( $d = 13.2 \mu\text{m}$ ;  $D = 29.6 \mu\text{m}$ ).

Experimental  $v(\sigma_a)$  dependence exhibits decreasing of DW velocity,  $v$ , with applied stresses,  $\sigma_a$  (Fig. 1.16a), but this dependence does not fit well with inverse square root dependence on applied stress (Fig. 1.16b). Here we plotted obtained experimentally dependences as  $\sigma_a(v^{-2})$ . From Fig. 1.16b we can conclude that obtained  $v(\sigma_a)$  dependences cannot be described by single  $v(\sigma_a^{-1/2})$  dependence. One of possible reasons of such deviation from predicted dependence is that when applied stresses are of the same order, as the internal stresses with complex tensor

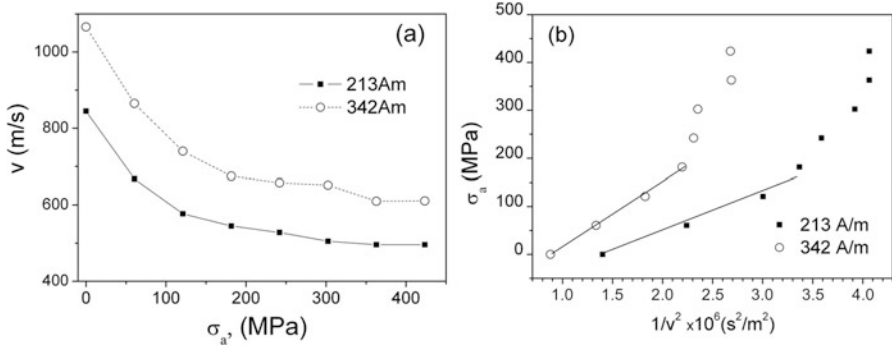


**Fig. 1.16**  $v(\sigma_a)$  dependences of  $\text{Fe}_{55}\text{Co}_{23}\text{B}_{11.8}\text{Si}_{10.2}$  microwires ( $d = 13.2 \mu\text{m}$ ;  $D = 29.6 \mu\text{m}$ ) (a) and  $\sigma_a(1/v^2)$  dependence (b). Reprinted with permission from [46]

character [46]. The other reason can be related with stress dependence of magnetostriction previously observed in various amorphous alloys [46].

Consequently DW dynamics in as-prepared Fe-rich and annealed Co-rich samples measured under stress have been compared.

As can be appreciated from Fig. 1.17, a typical nearly linear growth of DW velocity has been observed in as-prepared Fe-rich and annealed Co-rich samples measured without stress.

Under applied stress drastic decreasing of DW velocity has been observed in Fe-rich microwires. On the other hand, in Co-rich microwires increasing of DW velocity takes place (Fig. 1.17).

We observed that annealing performed at  $300^\circ\text{C}$  for 60 min in  $\text{Fe}_{74}\text{B}_{13}\text{Si}_{11}\text{C}_2$  microwire considerably affects  $v(H)$  dependence: DW velocity measured at the same magnetic field considerably increases, the range of fields where linear  $v(H)$  dependence takes place is extended and DW mobility,  $S$ , increased from  $4.02$  to  $4.65 \text{ m}^2/\text{As}$  (Fig. 1.17).

For explaining of the unusual features of Co-rich microwires with induced magnetic bistability we must consider that the origin of the magnetic bistability of amorphous glass-coated microwires is usually related to the fast magnetization switching of a large single axially magnetized domain [1]. In the case of Fe-rich microwires with spontaneous magnetic bistability is considered that large axially magnetized single domain is surrounded by the outer radially magnetized shell. This domain structure is determined by the stresses arising during the rapid solidification of the microwire [1, 54, 55].

In the case of the microwires with spontaneous magnetic bistability the annealing does not affect the character of hysteresis loop but considerably affects the DW dynamics. Thus annealing performed at  $300^\circ\text{C}$  for 60 min in  $\text{Fe}_{74}\text{B}_{13}\text{Si}_{11}\text{C}_2$  microwire considerably affects  $v(H)$  dependence: DW velocity measured at the same magnetic field considerably increases, the range of fields

**Fig. 1.17** Applied stress dependence of DW velocity of as-prepared  $\text{Fe}_{70}\text{B}_{15}\text{Si}_{10}\text{C}_5$  and annealed at  $T_{\text{ann}} = 300^\circ\text{C}$  for 45 min  $\text{Co}_{69.2}\text{Fe}_{4.1}\text{B}_{11.8}\text{Si}_{13.8}\text{C}_{1.1}$  microwire. Reprinted with permission from [55]

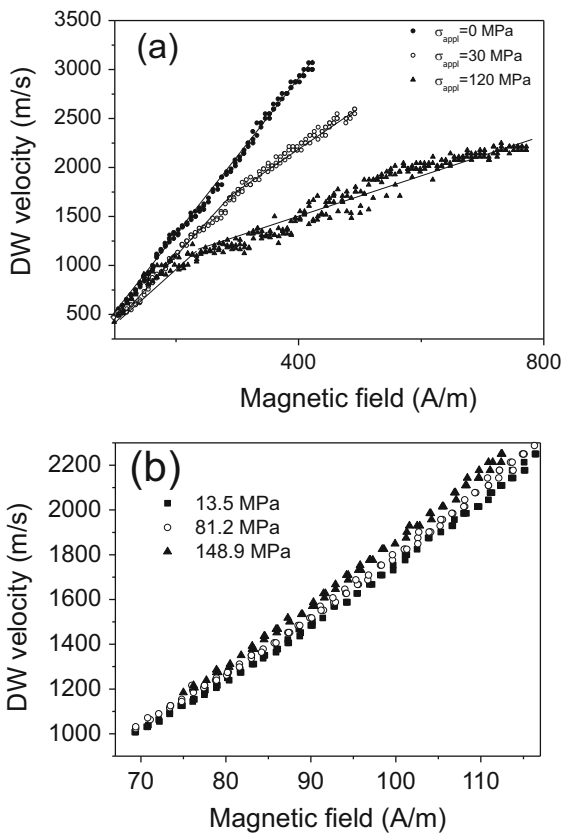
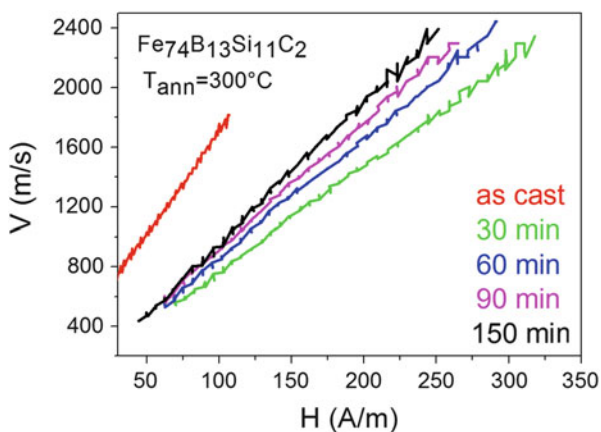


**Fig. 1.18** Effect of annealing on  $v(H)$  dependence of  $\text{Fe}_{74}\text{B}_{13}\text{Si}_{11}\text{C}_2$  microwire ( $d = 14.6 \mu\text{m}$ ,  $\rho = 0.55$ ). Reprinted with permission from [50]



where linear  $v(H)$  dependence takes place is extended and DW mobility,  $S$ , increased from 4.02 to 4.65 m<sup>2</sup>/As (Fig. 1.18).

Observed influence of sample annealing on DW dynamics in microwires with spontaneous magnetic bistability has been interpreted considering, partial internal stresses relaxation [50].

Increasing the annealing temperature above the crystallization temperature partial or complete crystallization can be achieved. Usually crystallization results in drastic magnetic hardening and deterioration of magnetic properties, but in some cases magnetic softness can be enhanced.

### 1.3 Effect of Partial Crystallization and Nanocrystallization on Magnetic Properties and GMI

As mentioned above although crystallization of amorphous materials usually results in degradation of their magnetic softness, in some cases crystallization can improve magnetically soft behaviour. This is the case of the so-called nanocrystalline alloys obtained by suitable annealing of amorphous metals. These materials have been introduced in 1988 by Yoshizawa and Yamauchi [28] and later have been intensively studied by a number of research groups [29–31]. As mentioned in the introduction the nanocrystalline structure of partially crystalline amorphous precursor is observed particularly in Fe-Si-B with small additions of Cu and Nb. Small additions of Cu and Nb allow inhibiting of the grains nucleation and decreasing of the grain growth rate [29–31]. Main interest in such nanocrystalline alloys is related to extremely soft magnetic properties combined with high saturation magnetization. Such soft magnetic character is thought to be originated because the magnetocrystalline anisotropy vanishes and the very small magnetostriction value when the grain size approaches 10 nm [28–31].

Recently considerable improvement of GMI effect in the case of glass-coated microwires is reported quite recently [34–37].

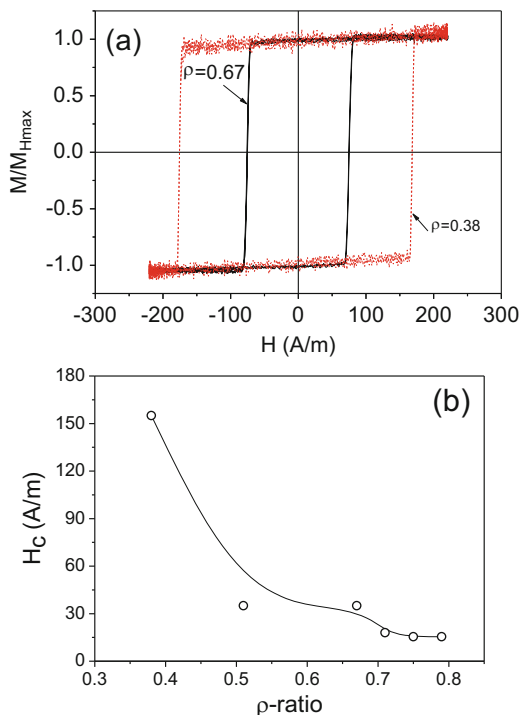
As-prepared Finemet-type  $\text{Fe}_{73.4}\text{Cu}_1\text{Nb}_{3.1}\text{Si}_x\text{B}_{22.5-x}$  ( $x = 11.5, 13.5$  and  $16.5$ ) and  $\text{Fe}_{73.4-x}\text{Cu}_1\text{Nb}_{3.1}\text{Si}_{13.4+x}\text{B}_{9.1}$  ( $0 \leq x \leq 1.1$ ) microwires present rectangular hysteresis loops similarly to other Fe-rich amorphous microwires [34–36]. For illustration in Fig. 1.19a the hysteresis loops of  $\text{Fe}_{70.8}\text{Cu}_1\text{Nb}_{3.1}\text{Si}_{14.5}\text{B}_{10.6}$  microwires with different  $\rho$ -ratios ( $\rho = 0.67$  and  $\rho = 0.38$ ) are provided.

The coercivity,  $H_c$ , of as-prepared Finemet-type microwires depends on ratio  $\rho = d/D$  (Fig. 1.19b).

Figure 1.20a, b, c presents XRD spectra of some selected as-prepared  $\text{Fe}_{70.8}\text{Cu}_1\text{Nb}_{3.1}\text{Si}_{16}\text{B}_{9.1}$ ,  $\text{Fe}_{70.8}\text{Cu}_1\text{Nb}_{3.1}\text{Si}_{14.5}\text{B}_{10.6}$  and  $\text{Fe}_{73.8}\text{Cu}_1\text{Nb}_{3.1}\text{Si}_{13}\text{B}_{9.1}$  microwires.

The first two peaks of the XRD spectra between 10° and 30° correspond to the glass layer and the other peaks at above 40° are related to the metallic nucleus. All

**Fig. 1.19** Hysteresis loops (a) and  $H_c(\rho)$  dependence (b) of  $\text{Fe}_{70.8}\text{Cu}_1\text{Nb}_{3.1}\text{Si}_{14.5}\text{B}_{10.6}$  as-prepared microwires. Reprinted with permission from [34]



$\text{Fe}_{70.8}\text{Cu}_1\text{Nb}_{3.1}\text{Si}_{16}\text{B}_{9.1}$  and  $\text{Fe}_{70.8}\text{Cu}_1\text{Nb}_{3.1}\text{Si}_{14.5}\text{B}_{10.6}$  samples present a completely amorphous structure (Figs. 1.20a, b).

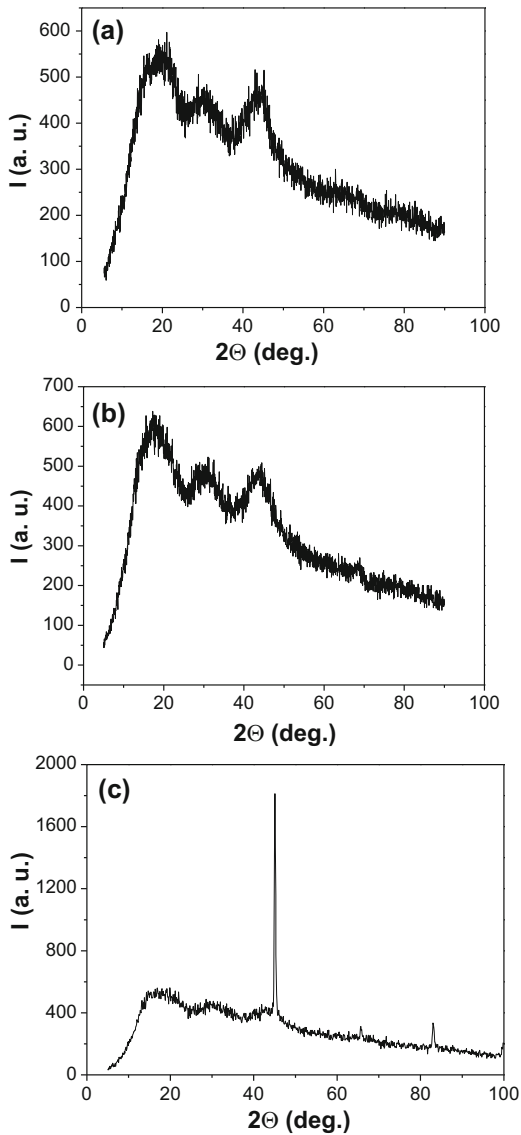
But some of  $\text{Fe}_{73.8}\text{Cu}_1\text{Nb}_{3.1}\text{Si}_{13}\text{B}_{9.1}$  microwires (see Fig. 1.20c) present a partially crystalline structure already in the as-prepared state.

Usually, the basic method to obtain a nanocrystalline structure from the amorphous state is achieving the crystallization of amorphous matrix by an appropriate heat treatment.

As-prepared samples have been annealed at different annealing temperatures,  $T_{ann}$ , for fixed annealing time. Annealing results in considerable changes of the structure and magnetic properties.

Starting from  $T_{ann}$  ranging from 550 to 650 °C a main crystalline peak is appearing in the range between 42° and 45° which corresponds to the existence of  $\alpha$ -Fe (Si) BCC crystal structure [34–36], as well as another two weak peaks appearing in the range between 65° and 85° (Fig. 1.21a). However, in the case of the  $\text{Fe}_{73.8}\text{Cu}_1\text{Nb}_{3.1}\text{Si}_{13}\text{B}_{9.1}$  microwire such crystalline peak has been observed in the as-prepared state (Fig. 1.21c) and consequently after annealing (Fig. 1.12b). Increasing the annealing temperature,  $T_{ann}$ , this peak is getting higher and narrower which indicates an increase in both the bcc-Fe phase volume fraction and grain size growth, respectively.

**Fig. 1.20** XRD patterns of as-prepared microwires:  $\text{Fe}_{70.8}\text{Cu}_1\text{Nb}_{3.1}\text{Si}_{16}\text{B}_{9.1}$  with  $\rho = 0.75$  (a),  $\text{Fe}_{70.8}\text{Cu}_1\text{Nb}_{3.1}\text{Si}_{14.5}\text{B}_{10.6}$  with  $\rho = 0.81$  (b) and  $\text{Fe}_{73.8}\text{Cu}_1\text{Nb}_{3.1}\text{Si}_{13}\text{B}_{9.1}$  with  $\rho = 0.6$  (c)



From the Debye–Scherrer equation (Eq. (1.7)), one can obtain the value of the grain size ( $D$ ).

$$D = k\lambda/\epsilon \cos 2\theta \quad (1.7)$$

where  $\epsilon$  is the half height width of the crystalline peak and  $2\theta$  is the angular position of the maximum crystalline peak. We found that the average grain size,  $D$ , in the

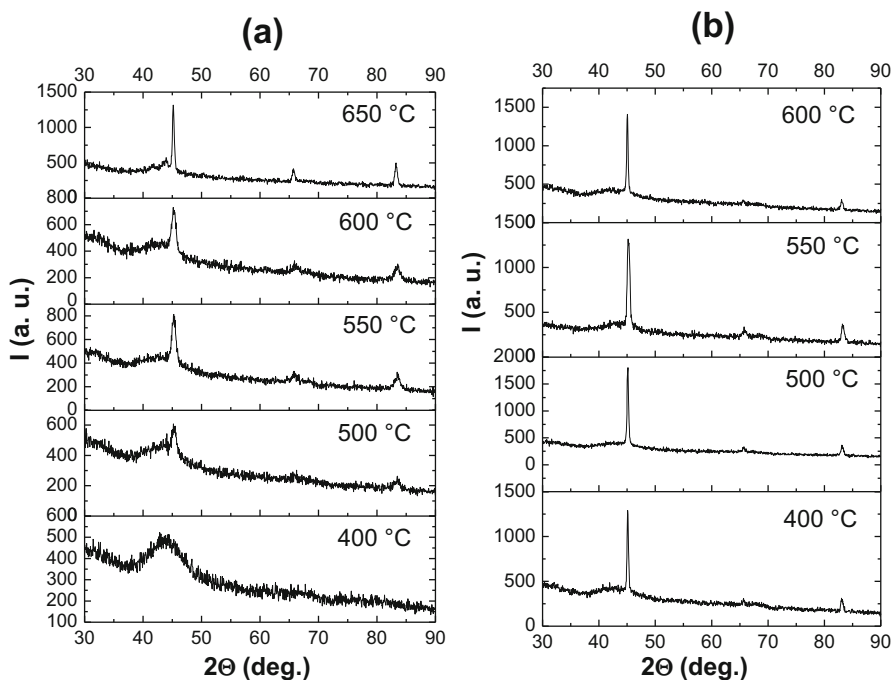
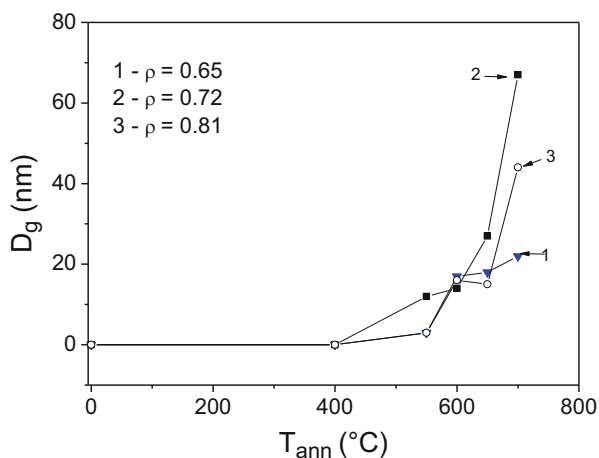


**Fig. 1.21** XRD patterns of annealed microwires  $\text{Fe}_{70.8}\text{Cu}_1\text{Nb}_{3.1}\text{Si}_{14.5}\text{B}_{10.6}$  with  $\rho = 0.81$  (a) and  $\text{Fe}_{73.8}\text{Cu}_1\text{Nb}_{3.1}\text{Si}_{13}\text{B}_{9.1}$  with  $\rho = 0.6$  (b). Annealing temperatures are indicated within each pattern

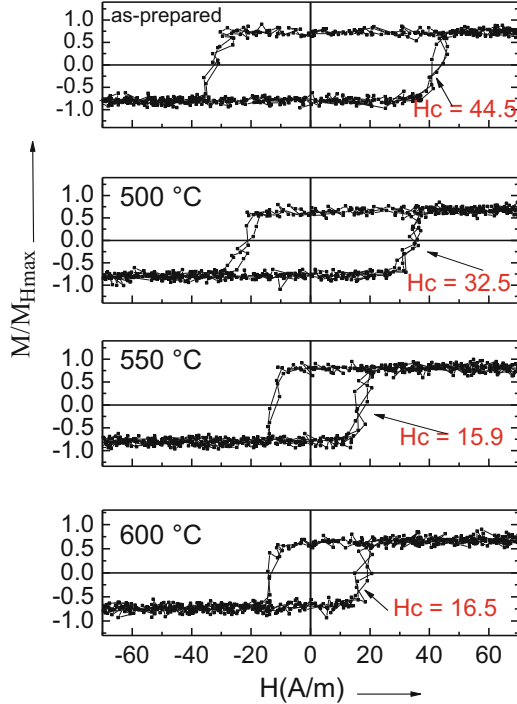
**Fig. 1.22** Dependence of average grain size on annealing temperature for  $\text{Fe}_{70.8}\text{Cu}_1\text{Nb}_{3.1}\text{Si}_{14.5}\text{B}_{10.6}$  microwires with various  $\rho$ -ratios



range of  $550 \text{ }^\circ\text{C} \leq T_{\text{ann}} \leq 600 \text{ }^\circ\text{C}$  is between 12 and 17 nm. By increasing  $T_{\text{ann}} \geq 650 \text{ }^\circ\text{C}$ ,  $D$  rapidly increases achieving values above 30 nm (see Fig. 1.22).

Strong dependence of magnetic properties on the sample's geometry in as-prepared state has been observed for all compositions. Hysteresis loops (plotted

**Fig. 1.23** Hysteresis loops of as-prepared and annealed  $\text{Fe}_{70.8}\text{Cu}_1\text{Nb}_{3.1}\text{Si}_{14.5}\text{B}_{10.6}$  microwires, with  $\rho = 0.81$ , at different temperatures measured at fixed magnetic field amplitude of 225 A/m



as the normalized magnetization  $M/M_{H_{\max}}$  versus applied magnetic field  $H$ ) of as-prepared microwires present rectangular shape typical for amorphous Fe-rich microwires (Fig. 1.19a). As can be appreciated from Fig. 1.19b the coercivity,  $H_c$ , is drastically affected by the  $\rho$ -ratio. Strong  $H_c(\rho)$  dependence can be explained taking into account the influence of the internal stresses on coercivity. As mentioned above the strength of internal stresses is a function of  $\rho$ -ratio.

Hysteresis loops of as-prepared and annealed  $\text{Fe}_{70.8}\text{Cu}_1\text{Nb}_{3.1}\text{Si}_{14.5}\text{B}_{10.6}$  microwires ( $\rho = 0.81$ ) at different temperatures are presented in Fig. 1.23. It is worth mentioning that the coercivity decreases upon increasing the annealing temperature, while the rectangular character of hysteresis loops is observed for all samples even annealed at below certain temperature.

In Fig. 1.24 we plotted coercivity dependence on annealing temperature for  $\text{Fe}_{70.8}\text{Cu}_1\text{Nb}_{3.1}\text{Si}_{14.5}\text{B}_{10.6}$  glass-coated microwire with different  $\rho$ -ratio.

According to these data, a tendency towards decreasing  $H_c$  values is observed at the range of 500–550 °C. Above  $T_{\text{ann}} \approx 600$  °C the magnetic bistability disappears (hysteresis loops cannot be considered perfectly rectangular). Similar behaviour associated with devitrification and magnetic softening has been previously reported in other Finemet-type microwires [34–36].

Consequently magnetic softening with lowest value of coercivity and switching field is obtained in the samples treated at 500–600 °C which could be ascribed to the



**Fig. 1.24** Dependence of the coercivity,  $H_c$ , for the  $\text{Fe}_{70.8}\text{Cu}_1\text{Nb}_{3.1}\text{Si}_{14.5}\text{B}_{10.6}$  glass-coated microwire with selected  $\rho$ -ratio on annealing temperature

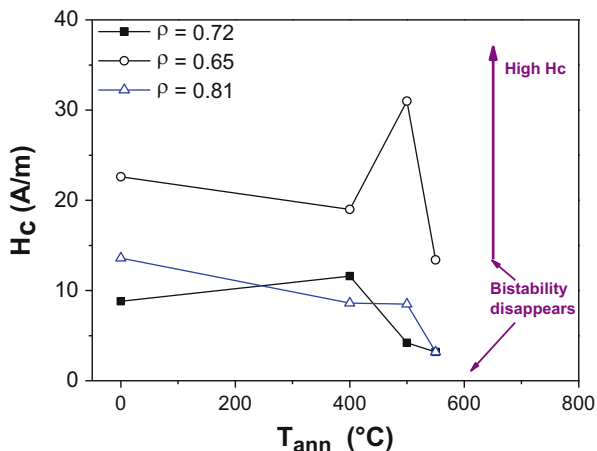
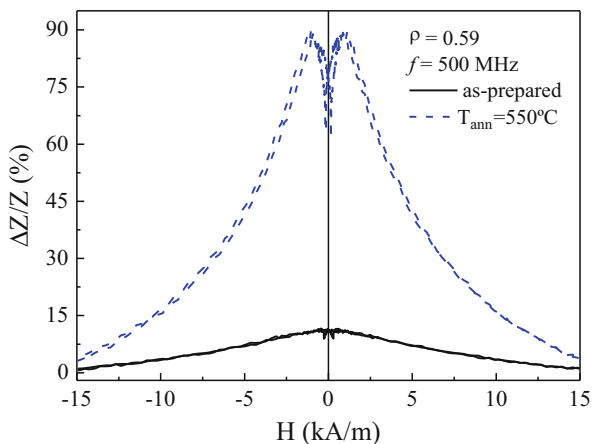


**Fig. 1.25** Effect of annealing at 550 °C for 1 h on  $\Delta Z/Z(H)$  dependence of  $\text{Fe}_{70.8}\text{Cu}_1\text{Nb}_{3.1}\text{Si}_{16}\text{B}_{9.1}$  microwire with  $\rho = 0.59$  measured at 500 MHz in comparison with the GMI response of the as-prepared sample



fact that the first crystallization process has been developed, leading to fine  $\alpha$ -Fe (Si) nanocrystals with grain size around 10–20 nm (compare Figs. 1.21 and 1.22). This behaviour is similar to that one widely reported for FINEMET ribbons [29–31].

GMI ration has been measured in as-prepared and annealed samples. As it was expected, samples with amorphous structure in as-prepared samples exhibit a rather small GMI effect (below 5 % see Fig. 1.25) similar to other Fe-based glass-coated microwires with positive magnetostriction. In contrast, nanocrystalline  $\text{Fe}_{70.8}\text{Cu}_1\text{Nb}_{3.1}\text{Si}_{16}\text{B}_{9.1}$  microwires annealed at 550 °C exhibit higher GMI effect ( $\Delta Z/Z \approx 90$  %, see Fig. 1.25).

Indeed like all Fe-based microwires, studied FeCuNbSiB microwires exhibit high positive magnetostriction. Consequently the stress distribution arising from simultaneous rapid quenching of metallic nucleus inside the glass coating must result in a longitudinal easy magnetization direction axis [1]. The resulting domain

structure (with low circular magnetic permeability typical for magnetically bistable samples) usually exhibits a small GMI effect. Therefore, GMI effect in the as-cast FINEMET microwires with positive magnetostriction is low.

A noticeable change in the GMI has been observed after the appearance of nanocrystallites (Fig. 1.25). As discussed elsewhere, after the nanocrystallization the average magnetostriction constant takes nearly zero values [29–31, 34–36], thanks to the control of the crystalline volume fraction:

$$\lambda_{s,\text{eff}} = V_{\text{cr}}\lambda_{s,\text{cr}} + (1 - V_{\text{cr}})\lambda_{s,\text{am}} \quad (1.8)$$

being  $\lambda_{s,\text{eff}}$  the saturation magnetostriction coefficient and  $V_{\text{cr}}$  the crystalline volume fraction.

The other family of microwires with nanocrystalline structure is the Hitperm-type microwires [59]. Hysteresis loops of all as-prepared microwires present rectangular shapes typical for Fe-rich amorphous microwires (see Fig. 1.26). As-prepared Hitperm-type microwires present much higher coercivity values as—compared with Finemet-type microwires (Fig. 1.26b). For comparison the microwires with similar  $\rho$ -ratio, i.e., with similar value of the internal stresses were compared.

In contrast to Finemet-type microwires, for as-prepared  $\text{Fe}_{38.5}\text{Co}_{38.5}\text{B}_{18}\text{Mo}_4\text{Cu}_1$  microwires ( $\rho = 0.6$ ) a noticeable peak appears at  $2\theta \approx 45^\circ$  that corresponds to  $\alpha$ -FeCo phase with an average grain size of about 33.3 nm randomly distributed in an amorphous matrix (Fig. 1.27b). The diffraction spectra must be attributed to the superposition of the peaks corresponding to the crystalline and amorphous phases.

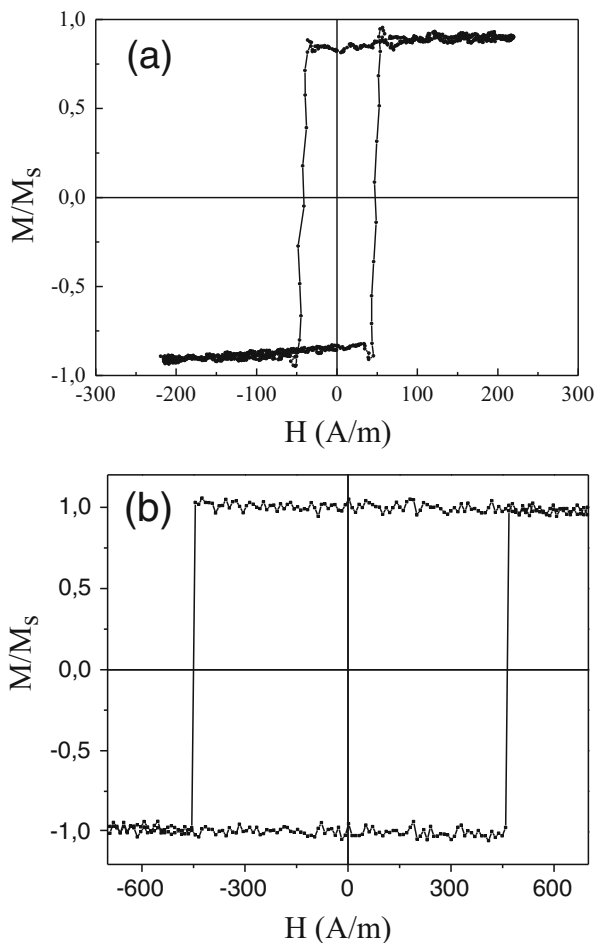
The nanocrystalline structure of  $\text{Fe}_{38.5}\text{Co}_{38.5}\text{B}_{18}\text{Mo}_4\text{Cu}_1$  microwires maintains after annealing at  $T_{\text{ann}} \leq 600^\circ\text{C}$  (with  $20 \leq D \leq 30$  nm).

It is worth mentioning that in contrast to Finemet-type nanocrystalline materials the magnetostriction of Hitperm-type materials remained highly positive due to the positive magnetostriction sign of the  $\alpha$ -FeCo nanocrystallites. Consequently, we measured (DW) velocities,  $v$ , of as-prepared and annealed Hitperm-type glass-coated microwires as shown in Fig. 1.28 where is presented as annealing affects to DW dynamics of  $\text{Fe}_{38.5}\text{Co}_{38.5}\text{B}_{18}\text{Mo}_4\text{Cu}_1$  microwires. Magnetic field range at which we observed single DW propagation becomes more extended in the annealed samples. This extended magnetic field region for single DW propagation must be related to stress relaxation and related magnetic softening observed after annealing.

Both as-prepared and annealed at  $450^\circ\text{C}$  samples present non-linear  $v(H)$  dependences. One of the possible explanations of such non-linearity could be attributed to the change of domain wall structure. The other reason for non-linearity can be associated with the defects [37, 46].

Consequently, after the devitrification of FINEMET and HITPERM-type microwires magnetic softness, enhanced GMI effect and high velocity of DW propagation can be observed.

**Fig. 1.26** Hysteresis loops of as-prepared  $\text{Fe}_{70.8}\text{Cu}_1\text{Nb}_{3.1}\text{Si}_{16}\text{B}_{9.1}$  microwires with  $\rho = 0.62$  (a) and  $\text{Fe}_{38.5}\text{Co}_{38.5}\text{B}_{18}\text{Mo}_4\text{Cu}_1$  with  $\rho = 0.60$  (b)



## 1.4 Conclusions

Studies of magnetic properties and GMI effect of amorphous Co–Fe-rich microwires reveal that selecting its appropriate chemical composition and geometry they present high GMI effect. Hysteresis loops and magnetic field dependences of GMI effect are affected by the magnetoelastic anisotropy.

Magnetic properties of amorphous microwires are strongly affected by the annealing. In Co-rich microwires after annealing rectangular hysteresis loops and coexistence of GMI effect and fast domain wall propagation can be observed. Observed changes are discussed considering effect of annealing on the magnetostriction coefficient. Similarly in Fe-rich microwires annealing affects the DW dynamics.

**Fig. 1.27** XRD patterns of Hitperm  $\text{Fe}_{38.5}\text{Co}_{38.5}\text{B}_{18}\text{Mo}_4\text{Cu}_1$  microwire ( $\rho \approx 0.6$ ) annealed at different temperatures for 1 h. Reprinted with permission from [59]

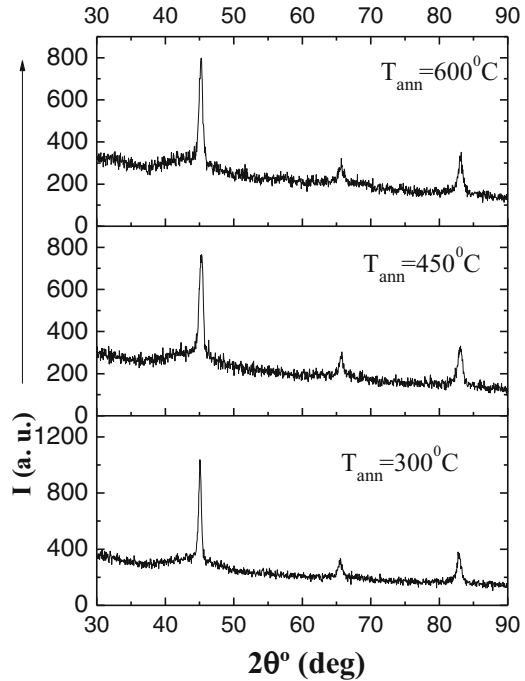
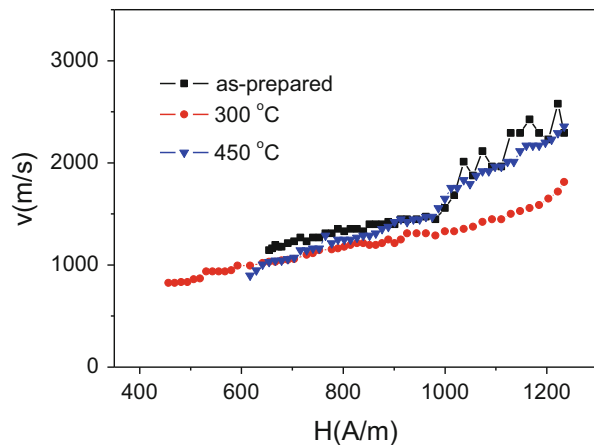


**Fig. 1.28** DW velocities dependences of magnetic field measured in as-prepared and annealed Hitperm  $\text{Fe}_{38.5}\text{Co}_{38.5}\text{B}_{18}\text{Mo}_4\text{Cu}_1$  microwires at different temperatures



Investigations of magnetic properties of Finemet-type Fe-Cu-Nb-Si-B microwires reveal that annealing considerably affects the hysteresis loops and GMI effect of this family of microwires. Magnetoelastic anisotropy affects soft magnetic properties of as-prepared FeCuNbSiB microwires. We observed magnetic softening and a considerable increasing of the GMI effect in Finemet-type FeCuNbSiB with nanocrystalline structure even in as-prepared microwires. After

an adequate annealing of Finemet-type microwires we observed a GMI ratio of about 100 %. The nanocrystallization of FeCuNbSiB microwires is a key factor for the optimization of the GMI effect.

In Hitperm-like  $\text{Fe}_{38.5}\text{Co}_{38.5}\text{B}_{18}\text{Mo}_4\text{Cu}_1$  microwires rectangular hysteresis loops and fast domain wall dynamics have been observed.

## References

1. Zhukova, V., Ipatov, M., Zhukov, A.: Thin magnetically soft wires for magnetic microsensors. *Sensors*. **9**, 9216–9240 (2009)
2. Phan, M.-H., Peng, H.-X.: Giant magnetoimpedance materials: fundamentals and applications. *Prog. Mater. Sci.* **53**, 323–420 (2008)
3. Zhukov, A., Zhukova, V.: *Magnetic Properties and Applications of Ferromagnetic Microwires with Amorphous and Nanocrystalline Structure*. Nova Science Publishers, New York (2009) ISBN: 978-1-60741-770-5
4. Chiriac, H., Corodeanu, S., Lostun, M., Ababei, G., Óvári, T.-A.: Magnetic behavior of rapidly quenched submicron amorphous wires. *J. Appl. Phys.* **107**, 09A301 (2010)
5. Chiriac, H., Ovari, T.A.: Amorphous glass-covered magnetic wires: preparation, properties, applications. *Prog. Mater. Sci.* **40**, 333 (1997)
6. Honkura, Y.: Development of amorphous wire type MI sensors for automobile use. *J. Magn. Mater.* **249**, 375–381 (2002)
7. Harrison, E.P., Turney, G.L., Rowe, H.: Electrical properties of wires of high permeability. *Nature*. **135**, 961 (1935)
8. Zhukov, A., Ipatov, M., Churyukanova, M., Kaloshkin, S., Zhukova, V.: Giant magnetoimpedance in thin amorphous wires: from manipulation of magnetic field dependence to industrial applications. *J. Alloys Compd.* **586**(Suppl. 1), S279–S286 (2014)
9. Panina, L.V., Mohri, K.: Magneto-impedance effect in amorphous wires. *Appl. Phys. Lett.* **65**, 1189–1191 (1994)
10. Beach, R.S., Berkowitz, A.E.: Giant magnetic-field dependent impedance of amorphous FeCoSiB wire. *Appl. Phys. Lett.* **64**(26), 3652 (1994)
11. Varga, R., Zhukov, A., Zhukova, V., Blanco, J.M., Gonzalez, J.: Supersonic domain wall in magnetic microwires. *Phys. Rev. B.* **76**, 132406 (2007). doi:[10.1103/PhysRevB.76.132406](https://doi.org/10.1103/PhysRevB.76.132406)
12. Ekstrom, P.A., Zhukov, A.: Spatial structure of the head-to-head propagating domain wall in glass-covered FeSiB microwire. *J. Phys. D: Appl. Phys.* **43**, 205001 (2010). doi:[10.1088/0022-3727/43/20/205001](https://doi.org/10.1088/0022-3727/43/20/205001)
13. Gudoshnikov, S.A., Grebenshchikov, Y.B., Ljubimov, B.Y., Palvanov, P.S., Usov, N.A., Ipatov, M., Zhukov, A., Gonzalez, J.: Ground state magnetization distribution and characteristic width of head to head domain wall in Fe-rich amorphous microwire. *Phys. Status Solidi A.* **206**(4), 613 (2009). doi:[10.1002/pssa.200881254](https://doi.org/10.1002/pssa.200881254)
14. Hayashi, M., Thomas, L., Retner, C., Moriya, R., Jiang, X., Parkin, S.: Dependence of Current and Field Driven Depinning of Domain Walls on Their Structure and Chirality in Permalloy Nanowires. *Phys. Rev. Lett.* **97**, 207205 (2006). doi:[10.1103/PhysRevLett.97.207205](https://doi.org/10.1103/PhysRevLett.97.207205)
15. Faulkner, C.C., Allwood, D.A., Cowburn, R.P.: Tuning of biased domain wall depinning fields at Permalloy nanoconstrictions. *J. Appl. Phys.* **103**, 073914 (2008). doi:[10.1063/1.2905318](https://doi.org/10.1063/1.2905318)
16. Larin, V.S., Torcunov, A.V., Zhukov, A., González, J., Vazquez, M., Panina, L.: Preparation and properties of glass-coated microwires. *J. Magn. Mater.* **249**(1-2), 39–45 (2002)
17. Taylor, G.F.: *Phys. Rev.* **24**, 6555–6560 (1924)
18. Ulitovskii, A.V., Maianski, I.M., Avramenko, A.I.: Author's Certification Patent No. 128,427, 3 Sept 1950

19. Wiesner, H., Schneider, J.: Structure transformation in Fe-based amorphous alloy. *Phys. Status Solidi A*. **32**(2), 655–659 (1975)
20. Wiesner, H., Schneider, J., Gemperle, R.: Annealing effects on the magnetic properties of rapidly quenched transition metal alloys. *Phys. Status Solidi A*. **36**(1), K59 (1976)
21. Gemperle, R., Kraus, L., Schneider, J.: Magnetization reversal of amorphous Fe<sub>80</sub>P<sub>10</sub>B<sub>10</sub> microwires. *Czech. J. Phys. B*. **28**, 1138 (1978)
22. Kraus, L., Schneider, J., Wiesner, H.: Ferromagnetic resonance in amorphous alloys prepared by rapid quenching from the melt. *Czech. J. Phys. B*. **26**, 601 (1976)
23. Kraus, L., Schneider, J.: Magnetostriction of Amorphous (Fe<sub>1-x</sub>Ni<sub>x</sub>)<sub>80</sub>P<sub>10</sub>B<sub>10</sub> Alloys. *Phys. Status Solidi A*. **39**, K161 (1977)
24. Zhukov, A., Zhukova, V.: *Magnetic Sensors Based on Thin Magnetically Soft Wires with Tuneable Magnetic Properties and its Applications*. International Frequency Sensor Association (IFSA) Publishing, Ronda de Ramon Otero Pedrayo (2014). ISBN-10: 84-617-1866-6
25. Konno, Y., Mohri, K.: Magnetostriction measurements for amorphous wires. *IEEE Trans. Magn.* **25**, 3623–3625 (1989)
26. Zhukov, A., Churyukanova, M., Kaloshkin, S., Sudarchikova, V., Gudoshnikov, S., Ipatov, M., Talaat, A., Blanco, J.M., Zhukova, V.: Magnetostriction of Co-Fe-based amorphous soft magnetic microwires. *J. Electron. Mater.* **45**, 226–234 (2015). doi:10.1007/s11664-015-4011-2
27. Zhukov, A., Zhukova, V., Blanco, J.M., Cobeño, A.F., Vazquez, M., Gonzalez, J.: Magnetostriction in glass-coated magnetic microwires. *J. Magn. Magn. Mater.* **258-259**, 151–157 (2003)
28. Yoshizawa, Y., Yamauchi, K.: Fe-based soft magnetic alloy composed of ultrafinegrain structure. *Mater. Trans. JIM*. **31**, 307–314 (1990)
29. Herzer, G.: Grain size dependence of coercivity and permeability in nanocrystalline ferromagnets. *IEEE Trans. Magn.* **26**, 1397–1402 (1990)
30. McHenry, M.E., Willard, M.A., Laughlin, D.E.: Amorphous and nanocrystalline materials for applications as soft magnets. *Prog. Mater. Sci.* **44**, 291–433 (1999)
31. Herzer, G.: Anisotropies in soft magnetic nanocrystalline alloys. *J. Magn. Magn. Mater.* **294**, 99–106 (2005)
32. Zhukova, V., Cobeño, A.F., Zhukov, A., Blanco, J.M., Larin V. and Gonzalez J.: Coercivity of glass-coated Fe<sub>73.4-x</sub>Cu<sub>1</sub>Nb<sub>3.1</sub>Si<sub>13.4+x</sub>B<sub>9.1</sub> (0 ≤ x ≤ 1.6) microwires. *Nanostruct. Mater.* **11**(8), 1319–1327 (1999)
33. Dudek, C., Adenot-Engelvin, A.L., Bertin, F., Acher, O.: *J. Non-Cryst. Solids*. **353**, 925 (2007)
34. Zhukov, A.P., Talaat, A., Ipatov, M., Blanco, J.M., Gonzalez-Legarreta, L., Hernando, B., Zhukova, V.: Effect of nanocrystallization on magnetic properties and GMI effect of microwires. *IEEE Trans. Magn.* **50**(6), 2501905 (2014)
35. Talaat, A., Zhukova, V., Ipatov, M., del Val, J.J., Gonzalez-Legarreta, L., Hernando, B., Blanco, J.M., Zhukov, A.: Effect of nanocrystallization on giant magnetoimpedance effect of Fe based microwires. *Intermetallics*. **51**, 59–63 (2014)
36. Talaat, A., Zhukova, V., Ipatov, M., Blanco, J.M., Gonzalez-Legarreta, L., Hernando, B., del Val, J.J., Gonzalez, J., Zhukov, A.: Optimization of the giant magnetoimpedance effect of Finemet-type microwires through the nanocrystallization. *J. Appl. Phys.* **115**, 17A313 (2014)
37. Chiriac, H., Ovari, T.A., Marinescu, C.S.: Giant magneto-impedance effect in nanocrystalline glass-covered wires. *J. Appl. Phys.* **83**, 6584 (1998)
38. Vázquez, M., Zhukov, A.: Magnetic properties of glass coated amorphous and nanocrystalline microwires. *J. Magn. Magn. Mater.* **160**, 223–228 (1996)
39. Usov, N.A., Antonov, A.S., Lagar'kov, A.N.: Theory of giant magneto-impedance effect in amorphous wires with different types of magnetic anisotropy. *J. Magn. Magn. Mater.* **185**, 159 (1998)
40. Pirola, K.R., Kraus, L., Chiriac, H., Knobel, M.: Magnetic properties and GMI in a CoFeSiB glass-covered microwire. *J. Magn. Magn. Mater.* **21**, L243–L247 (2000)

41. Zhukova, V., Chizhik, A., Zhukov, A., Torcunov, A., Larin, V., Gonzalez, J.: Optimization of giant magneto-impedance in Co-rich amorphous microwires. *IEEE Trans. Magn.* **38**(5), 3090–3092 (2002)
42. Velázquez, J., Vázquez, M., Zhukov, A.: Magnetoelastic anisotropy distribution in glass-coated microwires. *J. Mater. Res.* **11**, 2499–2505 (1996)
43. Antonov, A.S., Borisov, V.T., Borisov, O.V., Prokoshin, A.F., Usov, N.A.: Residual quenching stresses in glass-coated amorphous ferromagnetic microwires. *J. Phys. D: Appl. Phys.* **33**, 1161–1168 (2000)
44. Chiriac, H., Ovari, T.-A., Zhukov, A.: Magnetoelastic anisotropy of amorphous microwires. *J. Magn. Magn. Mater.* **254-255**, 469–471 (2003)
45. Zhukov, A., Ipatov, M., Zhukova, V.: Amorphous microwires with enhanced magnetic softness and GMI characteristics. *EPJ Web Conf.* **29**, 00052 (2012)
46. Zhukov, A., Blanco, J.M., Ipatov, M., et al.: Manipulation of domain wall dynamics in amorphous microwires through the magnetoelastic anisotropy. *Nanoscale Res. Lett.* **7**, 223 (2012). doi:[10.1186/1556-276X-7-223](https://doi.org/10.1186/1556-276X-7-223)
47. Zhukov, A.P., Vázquez, M., Velázquez, J., et al.: The remagnetization process of thin and ultrathin Fe-rich amorphous wires. *J. Magn. Magn. Mater.* **151**, 132–138 (1995)
48. Aragonese, P., Blanco, J.M., Dominguez, L., et al.: The stress dependence of the switching field in glass-coated amorphous microwires. *J. Phys. D: Appl. Phys.* **31**, 3040–3045 (1998)
49. Aragonese, P., Blanco, J.M., Cobeño, A.F., Dominguez, L., Gonzalez, J., Zhukov, A., Larin, V.: Stress dependence of the switching field in Co-rich amorphous microwires. *J. Magn. Magn. Mater.* **196-197**, 248–250 (1999)
50. Zhukov, A., Ipatov, M., Blanco, J.M., Chizhik, A., Talaat, A., Zhukova, V.: Fast magnetization switching in amorphous microwires. *Acta Phys. Pol., A.* **126**, 7–11 (2014)
51. Garcia-Prieto, M.J., Pina, E., Zhukov, A.P., et al.: Glass coated Co-rich amorphous microwires with improved permeability. *Sens. Actuators, A.* **81**(1-3), 227–231 (2000)
52. Zhukov, A., Gonzalez, J., Blanco, J.M., et al.: Induced magnetic anisotropy in Co-Mn-Si-B amorphous microwires. *J. Appl. Phys.* **87**, 1402–1408 (2000)
53. Zhukov, A., Vázquez, M., Velázquez, J., et al.: Frequency dependence of coercivity in rapidly quenched amorphous materials. *J. Mater. Sci. Eng. A.* **226-228**, 753–756 (1997)
54. Zhukov, A., Talaat, A., Ipatov, M., Blanco, J.M., Zhukova, V.: Tailoring of magnetic properties and GMI effect of Co-rich amorphous microwires by heat treatment. *J. Alloys Compd.* **615**, 610–615 (2014)
55. Zhukov, A., Talaat, A., Blanco, J.M., Ipatov, M., Zhukova, V.: Tuning of magnetic properties and GMI effect of Co-based amorphous microwires by annealing. *J. Electron. Mater.* **43**(12), 4532–4539 (2014). doi:[10.1007/s11664-014-3348-2](https://doi.org/10.1007/s11664-014-3348-2)
56. Zhukova, V., Ipatov, M., García, C., Gonzalez, J., Blanco, J.M., Zhukov, A.: Development of ultra-thin glass-coated amorphous microwires for high frequency magnetic sensors applications. *Open Mater. Sci. J.* **1**, 1–12 (2007)
57. Churyukanova, M., Semenkov, V., Kaloshkin, S., Shuvaeva, E., Gudoshnikov, S., Zhukova, V., Shchetinin, I., Zhukov, A.: Magnetostriction investigation of soft magnetic microwires. *Phys. Status Solidi A.* **213**, 363–367 (2016). doi:[10.1002/pssa.201532552](https://doi.org/10.1002/pssa.201532552)
58. Zhukov, A.: Design of magnetic properties of Fe-rich, glass-coated magnetic microwires for technical applications. *Adv. Funct. Mater.* **16**(5), 675–680 (2006)
59. Zhukova, V., Talaat, A., Ipatov, M., Del val, J.J., Blanco, J.M., Gonzalez-Legarreta, L., Hernando, B., Varga, R., Klein, P., Churyukanova, M., Zhukov, A.: Optimization of soft magnetic properties in nanocrystalline Fe-rich glass-coated microwires. *JOM.* **67**, 2108 (2015). doi:[10.1007/s11837-015-1546-x](https://doi.org/10.1007/s11837-015-1546-x)